AD-A260 742

ITATION PAGE

ed to average 1 hour per response, including the time for reviewing instructions, searching existing data sources, viewing the collection of information. Send comments regarding this burden estimate or any other aspect of this rden. to Washington Headquarters Services, Directorate for Information Operations and Reports, 1215 Jefferson fice of Management and Budget, Paperwork Reduction Project (0704-0188), Washington, DC 20503.

:T DATE 1/18/93	3. REPORT TYPE AND DATES COVERED *Technical*

4. TITLE AND SUBTITLE Design of Flexible Rods with Embedded SMA Actuators	5. FUNDING NUMBERS $DAAL03-92 G-0123$

6. AUTHOR(S)
H. James Pfaeffle, Dimitris C. Lagoudas,
Iradj Tadjbakhsh and Kevin C. Craig

7. PERFORMING ORGANIZATION NAME(S) AND ADDRESS(ES)

Rensselaer Polytechnic Institute
Dept. of Civil & Env. Engineering Dept.
JEC 4049
110 - 8th Street
Troy, NY 12180-3590

93-03103

DTIC
ELECTE
S FEB 18 1993
C D

9. SPONSORING/MONITORING AGENCY NAME(S) AND ADDRES

U. S. Army Research Office
P. O. Box 12211
Research Triangle Park, NC 27709-2211

SPONSORING/MONITORING GENCY REPORT NUMBER

$RO 30378.5-EG-URI$

11. SUPPLEMENTARY NOTES
The view, opinions and/or findings contained in this report are those of the author(s) and should not be construed as an official Department of the Army position, policy, or decision, unless so designated by other documentation.

12a. DISTRIBUTION/AVAILABILITY STATEMENT Approved for public release; distribution unlimited.	12b. DISTRIBUTION CODE

13. ABSTRACT (Maximum 200 words)

The shape change of a stress free cylindrical flexible rod with embedded SMA actuators is modeled in this paper for rods with single or multiple SMA actuators placed parallel to the long axis of the rod for the first heating the SMA actuators. The distributed axial compressive force, transverse normal force, and bending moments that act on the rod due to the shape recovery of the SMA actuators have been given by Lagoudas and Tadjbakhsh. The deformed shape of the rod is found by solving the nonlinear equations of equilibrium of the rod. For multiple actuators the resultant forces and moments are considered.

A design analysis is performed for the active rod with a single SMA actuator. Key design variables are E_{rod}, the thermal bond strength of the rod to the SMA actuator, and the rod dimensions. Key design parameters are: maximum rod/actuator interfacial shear stress, rod strain, rod slenderness ratio, and rod deflection. An analysis is then performed which investigates the influence of the design variables on each of the design parameters.

14. SUBJECT TERMS	15. NUMBER OF PAGES 12
	16. PRICE CODE

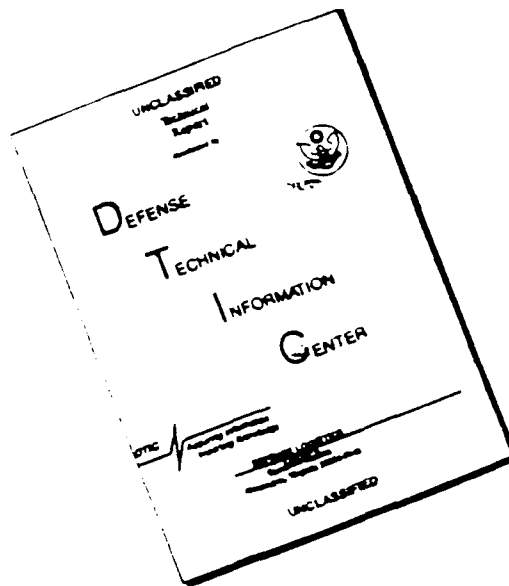| 17. SECURITY CLASSIFICATION OF REPORT UNCLASSIFIED	18. SECURITY CLASSIFICATION OF THIS PAGE UNCLASSIFIED	19. SECURITY CLASSIFICATION OF ABSTRACT UNCLASSIFIED	20. LIMITATION OF ABSTRACT UL

DISCLAIMER NOTICE

DEFENSE TECHNICAL INFORMATION CENTER

THIS DOCUMENT IS BEST QUALITY AVAILABLE. THE COPY FURNISHED TO DTIC CONTAINED A SIGNIFICANT NUMBER OF PAGES WHICH DO NOT REPRODUCE LEGIBLY.

Design of Flexible Rods with Embedded SMA Actuators

1. ABSTRACT

H. James Pfaeffle, Dimitris C. Lagoudas, Iradj G. Tadjbakhsh, Kevin C. Craig (Rensselaer Polytechnic Institute, Troy, NY 12180), (DL, Texas A & M Univ., College Station, TX 77843)

The shape change of a stress free cylindrical flexible rod with embedded SMA actuators is modeled in this paper for rods with single or multiple SMA actuators placed parallel to the long axis of the rod for the first heating the SMA actuators. The distributed axial compressive force, transverse normal force, and bending moments that act on the rod due to the shape recovery of the SMA actuators have been given by Lagoudas and Tadjbakhsh.[4,3] The deformed shape of the rod is found by solving the nonlinear equations of equilibrium of the rod. For multiple actuators the resultant forces and moments are considered.

A design analysis is performed for the active rod with a single SMA actuator. Key design variables are: E_{ROD}, the thermal bond strength of the rod to the SMA actuator, and the rod dimensions. Key design parameters are: maximum rod/actuator interfacial shear stress, rod strain, rod slenderness ratio, and rod deflection. An analysis is then performed which investigates the influence of the design variables on each of the design parameters. Optimal values are obtained which yield desired design parameter values. Experimental prototypes are fabricated, tested, and the deformed shape is compared to the theoretical prediction.

2. INTRODUCTION

In the field of active shape control using embedded shape memory alloy actuators, there are two methods of exerting forces on the host medium[1]. The first is through the use of embedded, sliding fibers that transmit normal forces distributed along their length and point follower forces at the ends of the fibers where the fibers are attached to the host medium. The second method is through the use of embedded, continuously bonded SMA actuators. These transmit distributed normal forces and distributed tangential forces through the interfacial shear stresses that develop in the actuator/host bond when the SMA recovery takes place. In this paper the second case of embedded, bonded SMA actuators is considered.

3. THEORY

The behavior of active rods with embedded SMA actuators is a result of the stress equilibrium that results when the SMA actuators are cyclically heated and cooled.[3] The following sequence of events occurs for the first heat/cool cycle:
1. The rod starts initially stress free.
2. Upon the first heating of the SMA actuators to the austenite phase, stress builds up in the SMA and the rod as a result of the fibers trying to recover their memory shape.
3. These stresses cause the rod to move to a new equilibrium shape.
4. Upon cooling, the SMA actuators are stretched out by the flexible rod through interfacial shear.

Upon cooling of the SMA actuators, the shape of the rod and the new memory strain imparted to the SMA actuators are a result of stress in the deformed rod stretching the reduced stiffness martensitic SMA actuators. A new stress equilibrium is established; the rod becomes less deformed and carries lower levels of stress. The SMA actuators get stretched out and acquire new, smaller memory strains. After this initial cooling, the rod will deform again when the SMA actuator is heated, but the deflection will be less than that achieved during the initial heating of the SMA actuators. This is due to a new stress equilibrium between the flexible rod and the increased stiffness austenitic SMA actuators trying to recover smaller memory strains. Subsequent heating/cooling cycles will not influence the residual stress states and the rod will cycle between first cooling and second heating shapes.

The stress in the SMA actuators that arises from the martensite to austenite phase transformation depends on the stiffness of the rod material. For a low stiffness rod, the stress in the SMA actuators remains below the yield strength of the austenitic SMA. However, if a rod is stiff enough, the yield strength of the austenitic SMA will be exceeded. The SMA actuators will acquire a new memory shape and even more actuator shape memory loss occurs. This must be kept in mind when modeling the forces generated in the active rod by an SMA actuator as a result of the phase transformations.

In this paper the problem of the first heating cycle is considered. The rod and actuators are initially stress free. To start, consider the problem of a flexible rod with a single SMA actuator embedded a distance d from the x_3 axis, placed at an angle θ from the x_1 axis, and parallel to the x_3 axis. The forces that act on the rod when the SMA actuator is heated and undergoes phase transition have been modeled by Lagoudas and Tadjbakhsh.[4,3] These forces are a distributed normal force, $\underline{f}_n$, and a distributed tangential force, $\underline{f}_t$. The rod has radius ρ and Young's modulus E while the SMA actuator has radius $ρ_a$ and Young's modulus E_a. The position of the SMA actuator referred to the body coordinate system of the rod is given by:

$$\underline{d} = d\cos\theta\,\underline{e}_1 + d\sin\theta\,\underline{e}_2 \qquad (1)$$

The body coordinate system of the rod is a coordinate system that follows the deformed rod. It has directions x_1 and x_2, which are in the principal directions of the rod; and x_3, which is orthogonal to x_1 and x_2. The problem appears below in Figure 1.
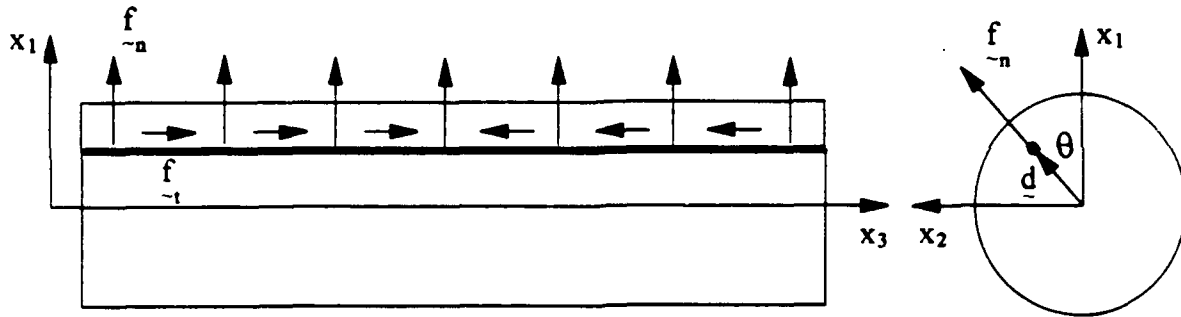

Figure 1. Body Coordinate System and Forces on an Active Rod

The shape of the rod is found by solving the nonlinear differential equations of equilibrium for inextensible thin rods along with the kinematic relations for a thin rod,[5,6,4,3] which take the following form:

Sum of Forces:

$$F_1' = -k_2F_3 + k_3F_2 - f_1 \qquad (2)$$
$$F_2' = -k_3F_1 + k_1F_3 - f_2 \qquad (3)$$
$$F_3' = -k_1F_2 + k_2F_1 - f_3 \qquad (4)$$

Sum of Moments:

$$M_1' = -k_2M_3 + k_3M_2 + F_2 - m_1 \qquad (5)$$
$$M_2' = -k_3M_1 + k_1M_3 - F_1 - m_2 \qquad (6)$$
$$M_3' = -k_1M_2 + k_2M_1 - m_3 \qquad (7)$$

Kinematic Relations:

$$x_1' = \sin\phi_2 \qquad (8)$$
$$x_2' = -\sin\phi_1\cos\phi_2 \qquad (9)$$
$$x_3' = \cos\phi_1\cos\phi_2 \qquad (10)$$

$$k_1 = \phi_1'\cos\phi_2\cos\phi_3 + \phi_2'\sin\phi_3 \qquad (11)$$
$$k_2 = \phi_2'\cos\phi_3 - \phi_1'\cos\phi_2\sin\phi_3 \qquad (12)$$
$$k_3 = \phi_3' + \phi_1'\sin\phi_2 \qquad (13)$$

Where F_1, F_2 and F_3 are the two shear forces and the axial force in the rod, respectively. k_1, k_2 and k_3 are the two curvatures and twist of the deformed rod per unit undeformed length, respectively. M_1, M_2, and M_3 are the two bending moments and torque in the rod, respectively. f_1, f_2 and f_3 are the distributed forces in the x_1, x_2 and x_3 directions, and m_1, m_2 and m_3 are the distributed moments in the x_1, x_2 and x_3 directions. These have been found by Lagoudas & Tadjbakhsh[4,3] and the following equations, (14)-(38), apply:

Vector Equations of Equilibrium for the SMA Actuator

$$\frac{d\underline{F}^a}{dZ} + \underline{f}^a = \left(\frac{dF^a}{dZ} + f_t^a\right)\underline{t} + (F^a k + f_n^a)\underline{n} = 0 \qquad (14)$$

Where:

$\underline{F}^a = F^a\,\underline{t}$ \qquad (15) - is the internal force in the actuator, which acts tangential to its center line

$\underline{f}^a = f_n^a\,\underline{n} + f_t^a\,\underline{t}$ \qquad (16) - is the distributed force acting on the actuator which has components normal and tangential to its center line

$$k = \sqrt{\frac{d\underline{t}}{dZ} \cdot \frac{d\underline{t}}{dZ}} \qquad (17) \text{ - is the actuator curvature per unit undeformed length}$$

$\underline{t}$ - is the unit vector tangent to the center line of the actuator, and is given by:

$$\underline{t} \equiv \frac{d\underline{x}}{dz} = \left(\frac{dz}{dS}\right)^{-1}\left[\left(\frac{dd_1}{dS} - d_2 k_3\right)\underline{e}_1 + \left(\frac{dd_2}{dS} + d_1 k_3\right)\underline{e}_2 + (1 + e - d_1 k_2 + d_2 k_1)\underline{e}_3\right] \qquad (18)$$

Where:

$\underline{x}$ - is the position vector of the deformed centroidal line of the rod, in Lagrangian coordinates

z - is deformed arc length along the actuator

S - is undeformed arc length along the centroidal line of the rod

e - is the extensibility of the rod

$$\frac{dz}{dS} = \left[(1 + e - d_1 k_2 + d_2 k_1)^2 + \left(\frac{dd_1}{dS} - d_2 k_3\right)^2 + \left(\frac{dd_2}{dS} + d_1 k_3\right)^2\right]^{1/2} \qquad (19)$$

For inextensible rods and zero applied twist, equations (18) & (19) reduce to: $\quad \underline{t} = \underline{e}_3 \qquad (20)$

$\underline{n}$ is the principal normal vector defined by: $\quad \underline{n} \equiv \frac{1}{k}\frac{d\underline{t}}{dZ} = \frac{1}{k}\frac{d\underline{t}}{dS}\left(\frac{dZ}{dS}\right)^{-1} \qquad (21)$

The deformed shape of the rod is defined by:

$$\frac{d\underline{e}_i}{dS} = \varepsilon_{kji} k_j \underline{e}_k \qquad (22) \qquad\qquad \text{Thus:} \qquad \frac{d\underline{t}}{dS} = k_2 \underline{e}_1 - k_1 \underline{e}_2 \qquad (23)$$

Also: $\quad \dfrac{dZ}{dS} = \sqrt{(1 - d_1 K_2 + d_2 K_1)^2 + \left(\frac{dd_1}{dS} - d_2 K_3\right)^2 + \left(\frac{dd_2}{dS} + d_1 K_3\right)^2} \qquad (24)$

Where: $\quad K_i$ - are the undeformed curvatures of the rod

$\quad\quad\quad\quad Z$ - is undeformed arc length along the actuator

For initially straight rods, (24) reduces to $\qquad \dfrac{dZ}{dS} = 1 \qquad (25)$

The actuator curvature, (17), takes the form: $\qquad k = \sqrt{k_1^2 + k_2^2} \qquad (26)$

The normal vector, (21), takes the form: $\qquad \underline{n} = \dfrac{k_2 \underline{e}_1 - k_1 \underline{e}_2}{\sqrt{k_1^2 + k_2^2}} \qquad (27)$

The normal force acting on the actuator from (14) and (16) reduces to:

$$\underline{f}^a_n = f^a_n \underline{n} = -F^a k \underline{n} = -F^a\left(k_2 \underline{e}_1 - k_1 \underline{e}_2\right) \qquad (28)$$

The axial force acting on the actuator is: $\qquad \underline{f}^a_t = -\dfrac{dF^a}{dS}\underline{e}_3 \qquad (29)$

The distributed force acting on the rod is coupled to the distributed force acting on the actuator through Newton's third law:

$$\underline{f}\, dS = -\underline{f}^a\, dZ \qquad (30)$$

The normal force acting on the rod is: $\qquad \underline{f}_n = -\underline{f}^a_n = F^a\left(k_2 \underline{e}_1 - k_1 \underline{e}_2\right) \qquad (31)$

The axial force acting on the rod is:
$$f_{-3} = -f_{-1} = \frac{dF^a}{dS} e_{-3}$$
(32)

Thus the distributed forces acting on the rod are given by:

$$f_1 = k_2 F^a \quad (33) \qquad f_2 = -k_1 F^a \quad (34) \qquad f_3 = \frac{dF^a}{dS} \quad (35)$$

The moments acting on the rod are given by:

$$m_{-1} = d_{-2} \times f_{-3} = d_2 f_3 e_{-1} \quad (36) \qquad m_{-2} = d_{-1} \times f_{-3} = d_1 f_3 e_{-2} \quad (37) \qquad m_{-3} = d \times f_{-n} = 0 \quad (38)$$

Note that for actuators placed parallel to the x_3 axis there is zero applied twist. F^a is the SMA actuation force, and has been found using a shear lag model solution[7] of the stress equations of equilibrium for the SMA actuator and rod, along with appropriate boundary and continuity conditions. This problem has been solved by Lagoudas & Tadjbakhsh.[4] Assuming that the SMA actuator stress remains in the elastic range, F^a takes the form:

$$F^a(S) = F^{SMA}\left(1 - \frac{e^{-\alpha S} + e^{-\alpha(L-S)}}{1 + e^{-\alpha L}}\right) \tag{39}$$

$$F^{SMA} = -\frac{\pi \rho_a^2 E \varepsilon_{SMA}}{\dfrac{E}{E_a} + \dfrac{\rho_a^2}{\rho^2 - \rho_a^2}} \quad (40) \qquad \alpha^2 = \frac{2G}{E \rho_a^2 \ln\left[(\rho - d)/\rho_a\right]}\left(\frac{E_2}{E_1} + \frac{\rho_a^2}{\rho^2 - \rho_a^2}\right) \quad (41)$$

The following constitutive assumptions are made[43] using beam theory:

$$M_1 = EI_{11}(k_1 - K_1) \quad (42) \qquad M_2 = EI_{22}(k_2 - K_2) \quad (43) \qquad M_3 = GI_{33}(k_3 - K_3) \quad (44)$$

For the case of an initially straight rod ($K_i = 0$) with a single SMA actuator placed parallel to the x_3 axis, there is no applied twist and the rod equilibrium equations and kinematic relations, (1)-(12), reduce to:

$$F_1' = -k_2 F_3 - f_1 \tag{45}$$
$$F_2' = k_1 F_3 - f_2 \tag{46}$$
$$F_3' = -k_1 F_2 + k_2 F_1 - f_3 \tag{47}$$

$$EI_{11}k_1' = F_2 - m_1 \tag{48}$$
$$EI_{22}k_2' = -F_1 - m_2 \tag{49}$$

$$x_1' = \sin\phi_2 \tag{50}$$
$$x_2' = -\sin\phi_1 \cos\phi_2 \tag{51}$$
$$x_3' = \cos\phi_1 \cos\phi_2 \tag{52}$$

$$\phi_1' = \frac{k_1}{\cos\phi_2} \tag{53}$$
$$\phi_2' = k_2 \tag{54}$$

These equations have been solved numerically[8] for the case of a simply supported rod with one SMA actuator with $\varepsilon_{SMA} = -.04$ placed at $\theta = \pi/4$, for the following rod parameter values: $E/E^a = 1/20$, $\rho^a/\rho = 1/10$, $d=1$, and $L=40$ cm. It is assumed that:
1. The SMA actuator offers little resistance to bending, and that its effect on rod stiffness is negligible; and 2. The stress in the SMA actuator does not exceed the yield strength of the austenitic SMA. Results appear below in Figure 2.
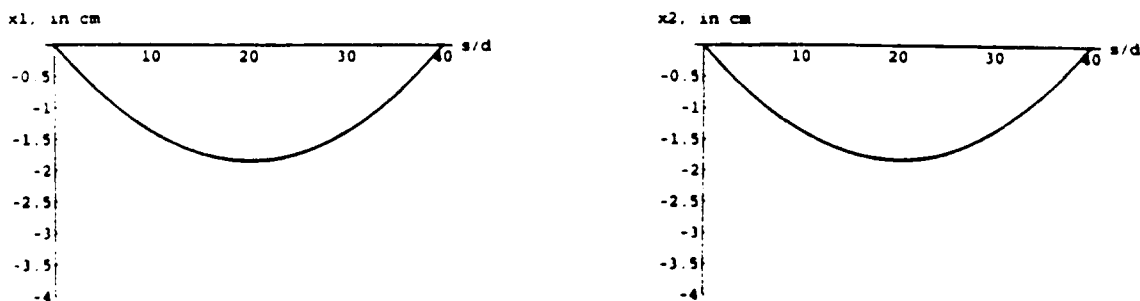

Figure 2. Deformed Shape of an Active Rod with a Single SMA Actuator Placed Parallel to the x_3 Axis

To extend this theory to the case of multiple SMA actuators, one must add the forces and moments imposed on the rod by each actuator to obtain resultant forces acting on the rod. Consider the case of two actuators, placed at angles θ_1 and θ_2 from the x_1 axis. For this problem it is be assumed that the SMA actuators are both martensistic with identical memory prestrains before heating. Like before, this analysis is conducted only for the first heating of the SMA actuators when the active rod is initially stress free, and it is assumed that the effect of embedded actuators on rod stiffness is negligible and that the stress in the actuator remains in the elastic range. This problem is illustrated below in Figure 3.
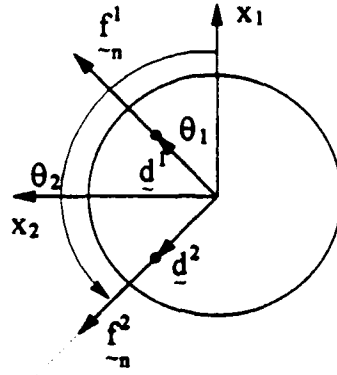

Figure 3. Distributed Normal Forces Acting on an Active Rod with 2 Embedded SMA Actuators

The resultant forces and moments acting on this rod are:

$$f_1 = k_2(F_1^a + F_2^a) \quad (55) \qquad f_2 = -k_1(F_1^a + F_1^a) \quad (56) \qquad f_3 = \frac{dF_1^a}{dS} + \frac{dF_2^a}{dS} \quad (57)$$

$$m_1 = d_2^1 f_3^1 + d_2^2 f_3^2 \quad (58) \qquad m_2 = -(d_1^1 f_3^1 + d_1^2 f_3^2) \quad (59)$$

Where the subscript on F^a and the superscript on f_3 refer to the actuator number. This problem has been solved numerically for the case of a simply supported rod with two embedded SMA actuators of equal diameter and $\varepsilon_{SMA} = -.04$, placed at $\theta_1 = \pi/4$, $\theta_2 = 3\pi/4$; for the same rod parameter values as for the single SMA actuator case. Results appear below in Figure 4.
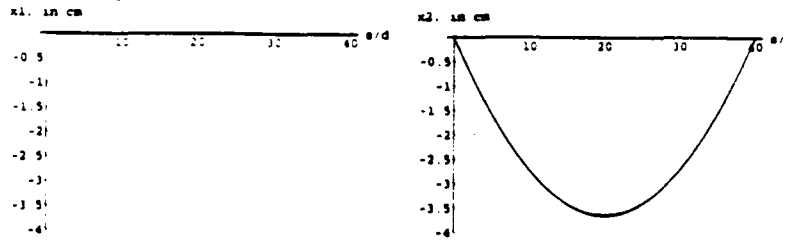

Figure 4. Deformed Shape of an Active Rod with Two SMA Actuators
Placed Parallel to the x_3 Axis at angles θ_1 and θ_2 from the x_1 Axis

This problem was also solved using the same values for all parameters except $\varepsilon^1_{SMA} = -.04$ and $\varepsilon^2_{SMA} = -.02$. Results appear below in Figure 5.
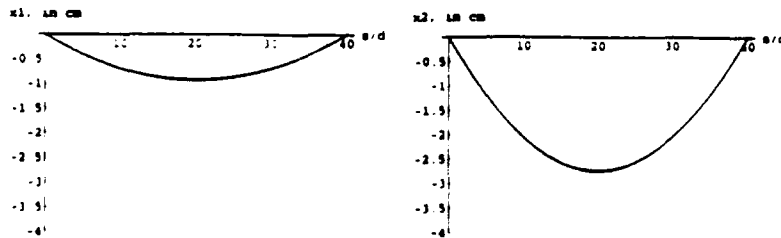

Figure 5. Deformed Shape of an Active Rod with Two SMA Actuators Placed Parallel to the x_3 Axis at angles θ_1 and θ_2 from the x_1 Axis and Prestrained to $\varepsilon^1_{SMA} = -.04$ and $\varepsilon^2_{SMA} = -.02$

4. DESIGN OF FLEXIBLE RODS WITH EMBEDDED, BONDED SMA ACTUATORS

A successful design is one that works dependably. In order to design successfully, one must arrive at key design specifications. The key design specifications were identified as:

1. Rod must be able to move to the desired shape.
2. Rod material must be compliant enough to carry the actuator/rod interfacial shear stress at levels lower than the material to heated SMA bond strength.
3. The maximum strain in the rod must not exceed the yield strain of the rod material.
4. The rod material must be able to be molded at temperatures below the transition temperature of the SMA actuators.
5. Rod slenderness ratio, ρ/L, should be less than 0.05 for beam theory to be a good constitutive assumption.
6. Stress in the SMA actuator should not exceed the yield stress of austenititic SMA for the elastic shape control theory[4,3] to hold.

To quantify these design specifications, several tasks were performed. The first was a parametric study of the influence of key model input variables on the maximum interfacial shear stress. The interfacial shear stress predicted by the shear-lag model of Lagoudas and Tadjbakhsh[4,7] for a SMA actuator of cross sectional area A^a is:

$$\bar{\tau_i} = F^{SMA} A_a \frac{\alpha \rho_a}{2} \left(\frac{e^{-\alpha(L-X_3)} - e^{-\alpha X_3}}{1 + e^{-\alpha L}} \right) \qquad (60)$$

The maximum interfacial shear stress occurs at the ends of the rod, $x_3 = 0$ or $x_3 = L$. The parametric study investigated the effects of changing rod radius, actuator radius, actuator placement distance, rod elastic modulus, rod length, and the actuator memory prestrain. To this end tensile testing was conducted on the polyurethane and silicone molding compounds. A Mathematica[8] program was written that plotted the maximum interfacial shear stress as a function of each parameter, while holding the other parameters constant at a given reference value. The reference values chosen were: $E_{SMA} = 70$ GPa, $E = 0.5$ GPa, $\rho_a = 1/5$ cm, $\rho = 5/3$ cm, $d = 1$ cm, $\varepsilon_{SMA} = -0.01$, and $L = 40$ cm. Results appear below in Figure 6.
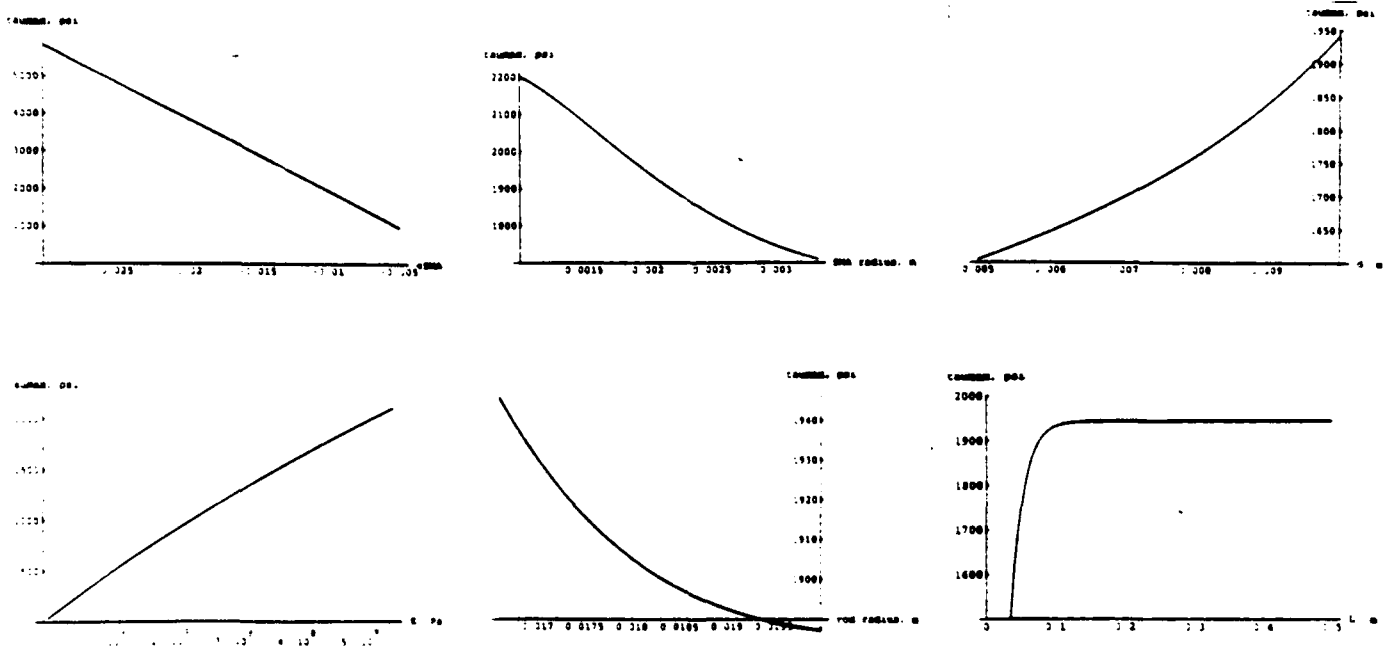

Figure 6. Plots of Maximum Interfacial Shear Stress in an Active Rod
as Design Parameters are Varied

The next step in the design of an active rod was to search for materials. 55.1 wt% .045" diameter Nitinol wire was obtained courtesy of L.McD. Shetky and Memry Tech (Brookefield, CT). A review of thermoset and thermoplastic polymers revealed a few thermoset polymers that would satisfy the stiffness and room temperature processing needs. The polymers identified were polyurethane molding compounds, silicone molding compounds, and some epoxy formulations.

To evaluate these materials for SMA thermal bond characteristics, a pullout test was designed to measure approximate SMA thermal bond strength. Samples were obtained of a flexible polyurethane molding compound (TU900, CONAP, Olean, NY) and a silic   molding compound (RTV662, GE Silicones, Waterford, NY). Pullout testing was performed on these materials. It was found that although the polyurethane is known to bond to metal better than the silicone, under conditions of a heated SMA actuator the polyurethane debonded. It was decided to design the active rod using the silicone mold making compound. Materials testing was performed to determine its tensile properties.

The last stage in the design process was to iteratively run the theoretical shape control model[4,5] for a single SMA actuator aligned with the x_1 axis. The deformed rod shape, maximum interfacial shear stress, maximum rod strain, and the maximum actuator stress was evaluated with each iteration. Design values arrived at for the test rod are as follows:

$\rho_2 = 0.0225$ inches $E_a = 70$ GPa[9] $\varepsilon_{SMA} = -0.03$ d=0.5 inches

$\rho = 0.625$ inches $E = 237.33$ psi $L = 10.75$ inches

The motivation behind producing such a rod is to experimentally test the shape control theory of Lagoudas and Tadjbakhsh.[4,5] Work is under way to produce such a rod and measure its deformed shape during heating and cooling cycles. For such a rod, with a single SMA actuator placed at $\theta = 0$, the shape control theory of Lagoudas and Tadjbakhsh[4,5] predicts a maximum interfacial shear stress of 64.85 psi, a maximum strain of 0.09 and the shape shown below in Figure 7.
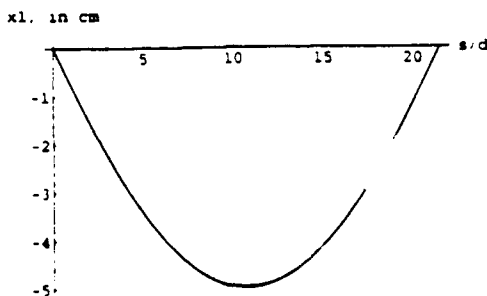

Figure 7. Shape of an Active Rod with a Single SMA Actuator
Placed Parallel to the x_1 Axis and Aligned with the x_1 Axis.

5. EXPERIMENTAL METHODS

5.1 Preparation of SMA Actuators

The first task in producing the experiment was preparation of SMA actuators from raw, as annealed, Nitinol wire. This wire was received in a coil. In order to insure that the actuators have a perfectly straight memory shape, it was decided to anneal the SMA while clamped in a straight configuration.

Once annealed, the SMA actuators must be carefully strained by the desired amount. To achieve these ends, a unique annealing and straining jig was designed and fabricated from steel. This jig was designed to clamp the SMA in a straight configuration and be heated in a furnace or used to stretch the SMA wire. A drawing of this jig appears below in Figure 8.
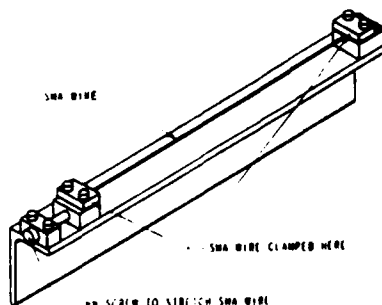

Figure 8. Anneal / Strain Jig for SMA Wire

using an Instron mechanical testing machine.[10] The slowest deformation rate, 0.1 in/min, was used. The test specimens had a gauge length of 1.25 inches and area 0.1 in^2.

5.4 Preparation of an Active, Flexible Rod with an Embedded SMA Actuator

To prepare this rod, techniques similar to pullout specimen preparation were followed. First, a mold was constructed that could easily come apart for demolding. A drawing of this mold appears on the next page in Figure 10. The SMA actuators were sandblasted, strained, primed, and clamped into the mold as before. The silicone molding compound was degassed under vacuum to remove entrapped gas bubbles.
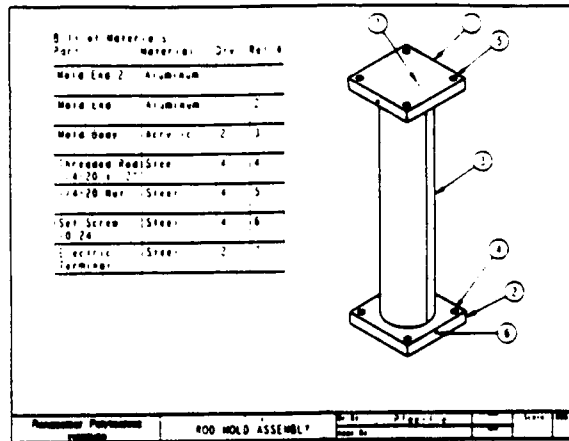

Figure 10. Mold for Preparation of Active Rods

5.5 Simple Supporting of an Active Flexible Rod

A system of simple supports was designed and built to simply support the rod for purposes of correlating to theory. The supports allow rotation at the ends of the rod, no displacement at $x_3 = 0$, and x_3 displacement only at $x_3 = L$. All rotating and sliding elements were designed to utilize ball bearings to reduce friction. The rod is attached to the simple supports using small wire ties, so that the fiber is aligned with the x_1 axis. A drawing of the experimental setup appears below in Figure 11.
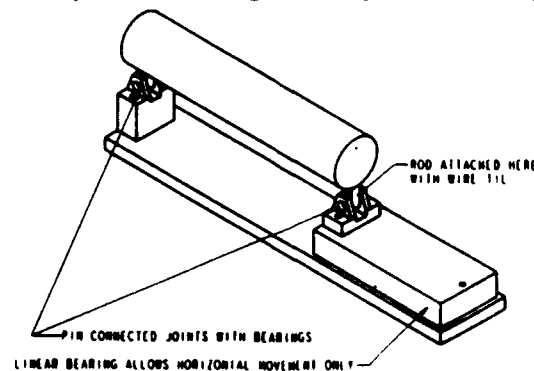

Figure 11. A Simply Supported Active Rod

5.6 Activation and Shape Measurement of an Active, Flexible Rod

Work is underway to run the experiment of cyclically activating the rod and measuring the deformed shape when activated and cooled. The following experimental protocol will be employed:
1. Place rod in simple support fixture.
2. Clamp simple support fixture into a Microvalidator Coordinate Measuring Machine.[11]
3. Pass just enough current through SMA using a variable AC transformer to achieve the phase transformation.
4. Measure the deformed shape of the activated rod.

The following protocol was used to prepare SMA actuators:
1. The SMA wire was cut into 1 foot lengths and clamped into the jig .
2. Annealed at 600 degrees C for 1/2 hour in the local steel treater's furnace (Steel Treaters, Troy, NY).
3. Strain SMA actuators by stretching and measuring twinned deformation.

5.2 Thermal Pullout Testing

The next step was to evaluate polyurethane and silicone molding compounds for SMA actuator bond strength. A pullout jig was designed to fit an Instron mechanical testing machine.[10] The pullout jig was designed to accept variable thickness, 0.75 inch diameter pullout specimens, and to constrain them in the axial direction during pullout. A schematic of the pullout test appears below in Figure 9.
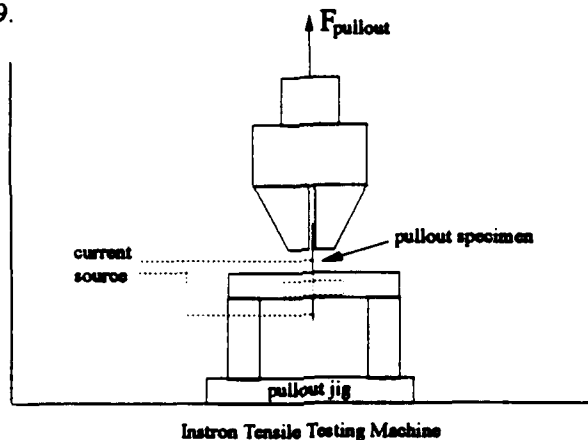

Instron Tensile Testing Machine

Figure 9. Schematic of Thermal Pullout Test

Pullout specimen thickness was arrived at based on the elasticity of the austenitic SMA actuator. Simple calculations revealed that a thickness of 0.25 inches prevented any appreciable elastic deformation of the actuator based on an estimated average bond strength of 500 psi. Pullout specimens were prepared using the following protocol:
1. Sandblast the annealed SMA actuators (accomplished by constraining SMA wire in a wood jig with a 1 mm wide slot to hold the SMA wire in place).
2. Strain SMA actuator to 5 % .
3. Prime SMA actuator with the appropriate metal bond strength enhancing primer (obtained from the polyurethane and silicone manufacturers).
4. Cut SMA actuators to a length of 4 inches.
5. Prepare pullout specimens by molding in a two-part mold.

The finished pullout specimen was a cylinder of diameter 0.75", height 0.25" with an SMA actuator embedded coaxially. The SMA actuator was fixed in place by a small clamp during molding. All molding compounds were degassed under vacuum both when in the mixing container and in the mold, to remove any air bubbles that form in the chemical curing process. In all, three pullout specimens of each material (TU900 and RTV662) were prepared. After pullout specimen preparation, the pullout testing was conducted using the following protocol:
1. A 20 lb. load cell was used in the testing machine.
2. The ends of the SMA actuators embedded in the pullout specimens were coated with electric insulating varnish.
3. The pullout specimens were put into the pullout jig, and the SMA actuator was clamped into a small test grip.
4. Just enough electrical current was passed through the SMA actuator to achieve the phase transformation, using a variable AC transformer.
5. The SMA was allowed to heat until it the force it exerted reached a maximum, and then mechanically pulled out.
6. The pullout force vs. deflection plot was then analyzed to determine thermal bond characteristics.

5.3 Materials Testing of Molding Compounds

A tensile test specimen of the silicone polymer was prepared using molding techniques. Tensile test specimens of polyurethane molding compounds were obtained from CONAP (Olean, NY). Tensile testing was performed on the specimen

5. Allow to cool.
6. Measure the deformed shape of the cooled rod.
7. Repeat steps 3 - 6 to investigate the effect of cyclic heating/cooling on the rod's shape memory effect.

6. RESULTS

6.1 Thermal Pullout Testing

It was found that the silicone molding compound possesses good thermal bond characteristics, with a sharp, predicable debond that occurs at an average interfacial shear stress level of 210 psi. It was found that the polyurethane molding compound possesses poor thermal bond characteristics. No sharp debond occurred for this material; rather, a gradual, slipping type of debond occurred. Sample force vs. displacement plots of thermal pullout testing for polyurethane and silicone thermoset polymers are shown on the next page in Figures 12 and 13.
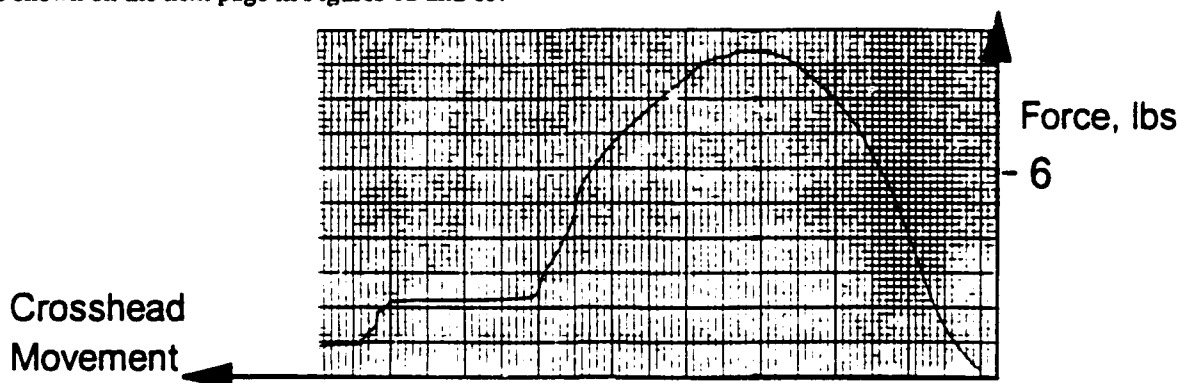

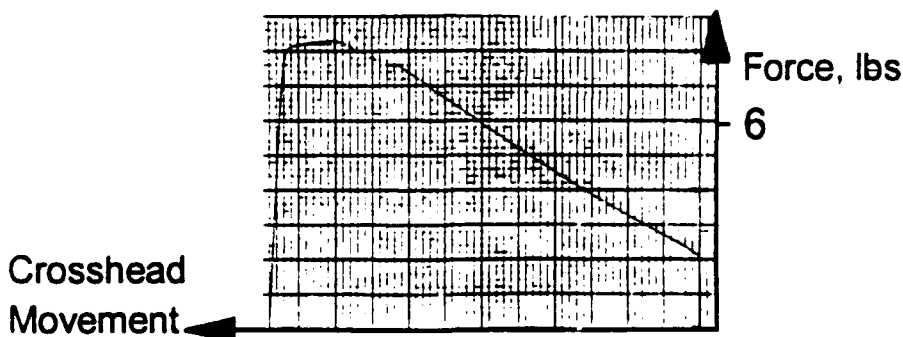Figure 12. Thermal Pullout Testing Results for Polyurethane TU900

Figure 13. Thermal Pullout Testing Results for Silicone RTV662

6.2 Tensile Testing of Silicone Molding Compound

The silicone molding compound was found to behave nonlinearly. A stress vs. strain curve appears below in Figure 14.
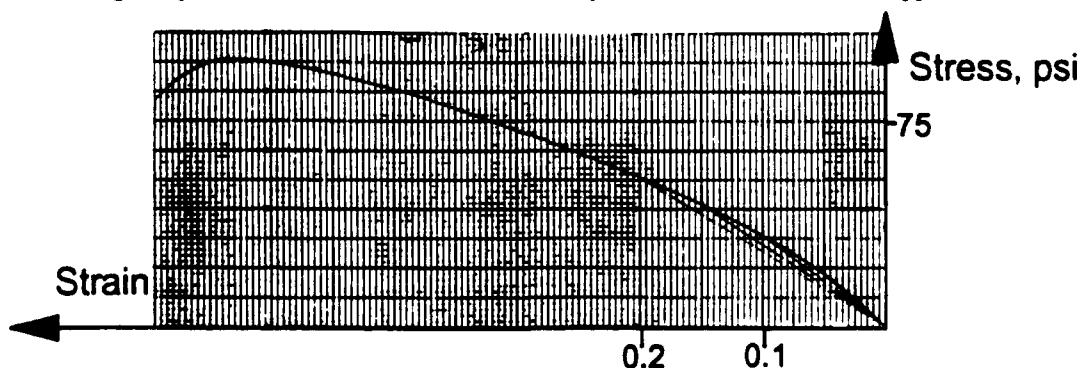

Figure 14. Stress vs. Strain Curve for RTV662 With Linear Sress-Strain Approximations Shown for $\varepsilon = 0.05, 0.10, 0.15,$ and 0.20.

7. DISCUSSION

The shape control theory[4,3] for multiple fibers predicts what one would expect. For two fibers that produce equal but opposite bending moments about the x_1 axis, no bending in the x_2 direction is predicted. But since these fibers produce a larger bending moment about the x_2 axis than a single fiber does, larger x_1 deflections are predicted compared to the case of a single fiber.

When ε_{SMA} is reduced in one of the two symmetrically placed SMA actuators, the two actuators no longer cancel bending moments about the x_1 axis, and a small x_2 deflection occurs in a direction opposite to the actuator possessing the larger ε_{SMA}. Since the overall bending moment about the x_2 axis is less, a smaller x_1 deflection is predicted compared to the case of two actuators possessing larger, equal ε_{SMA}.

The design of active rods with embedded, bonded SMA fibers is dictated by:
1. The bond strength of the host medium to the SMA actuator.
2. The processing temperature of the host medium.
3. The maximum host/actuator interfacial shear stress.

Two thermoset polymers were evaluated for thermal bond characteristics. It was found that the silicone molding compound bonded well to a heated SMA actuator. Pullout test results showed a sharp debond at an average stress level of 210 psi, indicated by a sharp leveling off in the pullout test force vs. displacement curve.

The polyurethane molding compound was found to possess poor thermal bond characteristics. In every case there was no sharp debonding of the SMA actuator. The force vs. displacement curve did not show a sharp leveling off and then a fast decline. Instead, the force vs. displacement curve rose and declined in a very linear, symmetric fashion. This behavior was attributed to sliding of the SMA actuator due to melting of the polyurethane host medium.

There are several possible sources of error in the theoretical analysis. The first source of error arises from the shear lag model solution for the forces applied to the SMA. It has been shown that the shear lag model mimics composite beam theory as actuator diameter becomes small and away from the ends of the beam.[3] Therefore, the relaxation of the SMA force that occurs as a result of bending the SMA actuator and rod together is taken into account away from the ends and for small diameter SMA actuators. The second source of error arises from treating the actuators as lines that do not increase the stiffness of the rod. This is a good approximation for one or two small diameter SMA actuators but becomes worse as the number of SMA actuators or actuator diameter is increased.

The third source of error in this analysis comes from assuming that the stress in the austenitic SMA actuator remains in the elastic range. One should check the stress in the actuator predicted by the shear-lag model[4,3] to insure that the analysis remains valid for the problem of interest. Note that the actuator stress stays in the elastic range only for very compliant host materials. Although it was not discussed in this paper, the current shape control theory of Lagoudas & Tadjbakhsh[4,3] handles yielding of the SMA with a change in the shear-lag model constitutive assumption for the austenitic SMA actuator from elastic to elastic, perfectly plastic. The last possible source of error arises from the use of beam theory for the constitutive assumptions. This approximation becomes worse as the slenderness ratio, ρ/L increases.

There were many possible sources of error in the experiment. In the preparation of SMA actuators, error could have been introduced in the measurement of the actuator twinned deformation and in the memory shape due to heating while sandblasting. In molding pullout specimens and active rods, error could have been introduced into the stress free initial condition and actuator placement while constraining the SMA actuator during molding. A small initial axial stress probably existed in the SMA actuator, because the SMA had to have a small amount of axial force exerted upon it to hold it at a constant distance from the x_3 axis during molding.

During pullout and tensile testing, small error could have been introduced into the axial force measured due to clamping the pullout or tensile specimen in the grips. Generally, this caused a small compressive force to be exerted. This was equilibrated by moving the Instron's crosshead slowly until the force readout neared zero. Any residual force was zeroed out using the force measurement zero control. In modeling the experiment, error could have been introduced into the constitutive assumptions by assuming elastic behavior for the silicone molding compound. This was handled by making a linear stress strain

approximation over the range of strain predicted by the shape control theory.[4,3] Also, since this was a static analysis, the tensile testing was conducted at the slowest deformation rate possible.

8. CONCLUSION

In this paper the behavior of active rods with embedded SMA actuators was addressed. An active rod loses some shape memory during the first heating/cooling cycle due to the fact that the flexible rod cannot stretch the martensitic actuator back to the original memory prestrain. Also, the yield strength of the austenitic SMA actuator can be exceeded if the stiffness of the rod material exceeds some critical value, which results in large actuator shape memory loss and complicates analytical modeling. The rod retains shape memory, but part of it results from residual stresses in the structure working against SMA actuator stiffness changes as the SMA undergoes phase transformation. All of these issues along with modeling of the subsequent heating/cooling cycles is covered in a paper currently under preparation by Lagoudas & Tadjbakhsh.[3]

It was shown that many different configurations for active shape control of flexible rods can be modeled using the theory of Lagoudas & Tadjbakhsh.[4,3] In particular, the problem of multiple embedded SMA actuators increases the range of shape control that is possible. A design analysis has revealed that the SMA actuator/host interfacial bond strength is one of the most critical design variables. A review of flexible polymers found that flexible thermoset materials which bond strongly to heated SMA actuators hold the most promise for active flexible rods with embedded, bonded SMA actuators. Work is underway to experimentally verify the active shape control theory of Lagoudas & Tadjbakhsh[4,3].

9. ACKNOWLEDGMENT

REFERENCES

1. Chaudry, Z. and Rogers, C.A., "Response of composite beams to internal actuator force", *Proceedings of the 31st Structures, Structural Dynamics, and Materials Conference*, AIAA-91-1166, 1991.

2. Buehler, W.J. and Wiley, R.C., "Nickel Based Alloys", U.S. Patent 3174, p. 851, 1965.

3. Lagoudas, D.C. and Tadjbakhsh, I.G., "Deformations of active flexible rods with embedded line actuators", (in preparation).

4. Lagoudas, D.C. and Tadjbakhsh, I.G., "Active flexible rods with embedded SMA fibers", *Smart Materials and Structures*, Vol.1, pp. 162-167, 1992.

5. Love, A.E.H., A Treatise on the Mathematical Theory of Elasticity, pp. 381-398, Dover, New York, 1944

6. Tadjbakhsh, I.G. and Lagoudas, D.C., "Variational theory of deformations of curved, twisted, and extensible elastic rods", *Journal of Elasticity*, (submitted).

7. Budiansky, B., Hutchinson, J.W., and Evans, A.G., "Matrix fracture in fiber reinforced ceramics", *J.Mech. Phys. Solids*, Vol. 34, 167-189, 1986.

8. Mathematica, Version 2.0, Wolfram Research, Inc., Champaign, IL, 1991.

9. Shetky, L. McD. and Wu, M.H., "The properties and processing of shape memory alloys for use as actuators in intelligent composite materials", *Smart Materials and Structures, ASME*, AD-Vol. 24/ AMD-Vol. 123, 1991.

10. Instron Universal Testing Machine, Instron Corporation, Canton, MA.

11. Microvalidator Coordinate Measuring Machine, Browne & Sharpe Mfg. Co., North Kingston, RI.